Molecular dissection of the ILK-PINCH-parvin triad reveals a fundamental role for the ILK kinase domain in the late stages of focal-adhesion maturation

Fabio Stanchi[1,2], Carsten Grashoff[2,*], Carine Flore Nguemeni Yonga[1,*], Dominique Grall[1], Reinhard Fässler[2] and Ellen Van Obberghen-Schilling[1,‡]

[1]Institute of Developmental Biology and Cancer Research, University of Nice-Sophia Antiopolis, CNRS-UMR6543, Centre Antoine Lacassagne, 33 Avenue de Valombrose, 06189 Nice, France
[2]Max Planck Institute of Biochemistry, Department of Molecular Medicine, 82152 Martinsried, Germany

*These authors contributed equally to this work
‡Author for correspondence (e-mail: vanobber@unice.fr)

Accepted 18 February 2009
Journal of Cell Science 122, 1800-1811 Published by The Company of Biologists 2009
doi:10.1242/jcs.044602

Summary

Integrin-linked kinase (ILK) and cytoplasmic adaptors of the PINCH and parvin families form a ternary complex, termed IPP, that localizes to integrin adhesions. We show here that deletion of the genes encoding ILK or PINCH1 similarly blocks maturation of focal adhesions to tensin-rich and phosphotyrosine-poor fibrillar adhesions (FBs) by downregulating expression or recruitment of tensin and destabilizing α5β1-integrin–cytoskeleton linkages. As IPP components are interdependent for integrin targeting and protein stability, functional dissection of the complex was achieved by fusing ILK, PINCH, parvin or their individual motifs to the cytoplasmic tail of β3 integrin, normally excluded from FBs. Using this novel gain-of-function approach, we demonstrated that expression of the C-terminal kinase domain of ILK can restore tensin recruitment and prompt focal-adhesion maturation in IPP-null cells. Debilitating mutations in the paxillin- or ATP-binding sites of ILK, together with α-parvin silencing, revealed a determinant role for ILK-parvin association, but not for direct paxillin binding, in this function. We propose a model in which the C-terminal domain of ILK promotes integrin sorting by reinforcing α5β1-integrin–actin linkage and controls force transmission by targeting tensin to maturing adhesions.

Supplementary material available online at
http://jcs.biologists.org/cgi/content/full/122/11/1800/DC1

Key words: Integrins, Cell adhesions, Integrin linked kinase

Introduction

Cell adhesion receptors of the integrin family assume fundamental roles throughout development and in adult organisms by mediating interactions between cells and the extracellular matrix that control migration, survival, proliferation, differentiation and matrix assembly (Hynes, 2002; van der Flier and Sonnenberg, 2001). To accomplish these diverse functions, integrins assemble a host of ancillary proteins into specialized adhesive structures with distinct morphologies, subcellular localization and signaling potential (Geiger et al., 2001). Focal complexes (FXs), focal adhesions (FAs) and fibrillar adhesions (FBs) are among the most widely studied, with FXs being the smallest adhesions that emerge from highly dynamic nascent adhesions (Choi et al., 2008) at the edge of extending lamellipodia and guide cell spreading. Shortly after their formation, FXs can either dissolve or connect to actin stress fibers and enlarge to form FAs that provide firm anchorage to the substrate. FBs, which are sites of fibronectin (FN) fibrillogenesis characterized by their elongated shape and more central location, are formed by translocation of α5β1 integrin dimers out of FAs along nascent FN fibers on the cell surface (Pankov et al., 2000; Zamir et al., 2000).

Several reports have described the diversity of these adhesive structures in terms of their composition, life span, integrin density and turnover, and dependence on acto-myosin-generated tension (Ballestrem et al., 2001; Zaidel-Bar et al., 2003; Zamir et al., 1999). With regard to their molecular content, the formation of FXs, FAs and FBs is accompanied by the hierarchical recruitment of different integrins and integrin-associated proteins (Zaidel-Bar et al., 2003). Typically, paxillin is recruited early into FXs, followed by vinculin, whereas zyxin and tensin are recruited after the complete maturation of FAs. The actin-binding protein tensin is particularly abundant in FBs, whereas levels of phosphotyrosine (PY) on resident proteins are significantly lower in these matrix-forming adhesions (Zamir et al., 1999).

Unraveling the signals that regulate the dynamic conversion of FXs to FAs and FBs is of primary importance for understanding integrin function. Previous studies from our laboratory have identified integrin-linked kinase (ILK) as a key regulator of the stability and/or turnover of FAs and FBs in fibroblasts and endothelial cells (Boulter et al., 2006; Vouret-Craviari et al., 2004). ILK is a modular scaffolding protein comprising an N-terminal array of ankyrin repeats, a short pleckstrin-homology (PH) domain and a C-terminal Ser/Thr kinase-like domain (Delcommenne et al., 1998). By means of its N-terminal ankyrin repeat, ILK binds to the first of five LIM domains in the adaptor protein PINCH1 (Chiswell et al., 2008; Li et al., 1999). In addition to integrin β subunits, the kinase domain interacts directly with other components of integrin-based adhesion plaques, including paxillin and the most C-terminal of the two calponin-homology (CH) domains of the adaptor protein α-parvin (also known as actopaxin and CH-ILKBP) (Nikolopoulos and Turner, 2002).

ILK, PINCH1 and α-parvin form a ternary complex termed IPP (ILK-PINCH-parvin) that localizes to both FAs and FBs and is

essential for several integrin-dependent functions (Legate et al., 2006; Wu, 2004). Formation of the IPP triad occurs before, and is a prerequisite for, recruitment of ILK, PINCH1 and α-parvin to integrin adhesions (Zhang et al., 2002), implying a functional interdependency of these proteins. ILK, PINCH1 and α-parvin proteins are also to a large extent interdependent for their stability as depletion of one leads to extensive proteasome-mediated degradation of the other two (Fukuda et al., 2003), thus rendering functional dissection of the complex difficult to achieve.

We show here that the IPP complex controls maturation of adhesions by stabilizing the integrin-actin connection and providing a permissive platform for tensin recruitment. Furthermore, using a novel gain-of-function strategy for molecular dissection of this complex, we identify the ILK C-terminus and α-parvin as essential partners in this process.

Results

ILK and PINCH1 are required for adhesion maturation

It has been shown in previous investigations that *ILK*$^{-/-}$ and *PINCH1*$^{-/-}$ fibroblasts exhibit fewer and smaller FA than parental *ILK*$^{fl/fl}$ and *PINCH1*$^{fl/fl}$ cells (Sakai et al., 2003; Stanchi et al., 2005). To explore the molecular basis of this phenotype, we analyzed the composition of *ILK*- and *PINCH1*-null adhesions by immunostaining. As adhesion maturation occurs through sequential recruitment of proteins (Zaidel-Bar et al., 2003), cells spreading on FN were stained with antibodies against the FN-binding α5β1 integrin and various 'early' and 'late' adhesion components.

In *ILK*$^{fl/fl}$ and *PINCH1*$^{fl/fl}$ cells, the peripheral FXs and FAs were rich in PY, paxillin and vinculin. Adhesions located more centrally contained lower levels of PY but were enriched in tensin1, consistent with the late recruitment of this protein during FA maturation (Fig. 1A; and F.S., unpublished results). Zyxin, described as a late FA component, was present in large FAs at the tips of thick stress fibers. In accordance with its role as a mechanosensitive protein (Yoshigi et al., 2005), zyxin could also be detected along actin microfilaments, as determined by phalloidin staining (D.G., unpublished results).

ILK-null cells were strikingly devoid of the tensin-rich central adhesions with low PY content. Instead, they formed a fringe of peripheral adhesions strongly staining for phosphotyrosine and containing the 'early' FA components paxillin and vinculin. Zyxin was only faintly visible in adhesions of the *ILK*-null cells and never present along stress fibres (Fig. 1A). *PINCH1*$^{-/-}$ cells exhibited an identical phenotype (D.G., unpublished results). Western blot analysis revealed a downregulation of both tensin1 and zyxin proteins after *ILK* or *PINCH1* deletion (Fig. 1B). Decreased protein expression was accompanied by a decrease in mRNA encoding tensin1 but not zyxin (Fig. 1C). Interestingly, tensin1 but not vinculin was detectable in ILK co-immunoprecipitates from *ILK*$^{fl/fl}$ lysates (Fig. 1D), suggesting that the IPP complex forms a tighter link with tensin1 than with components of 'early' adhesions.

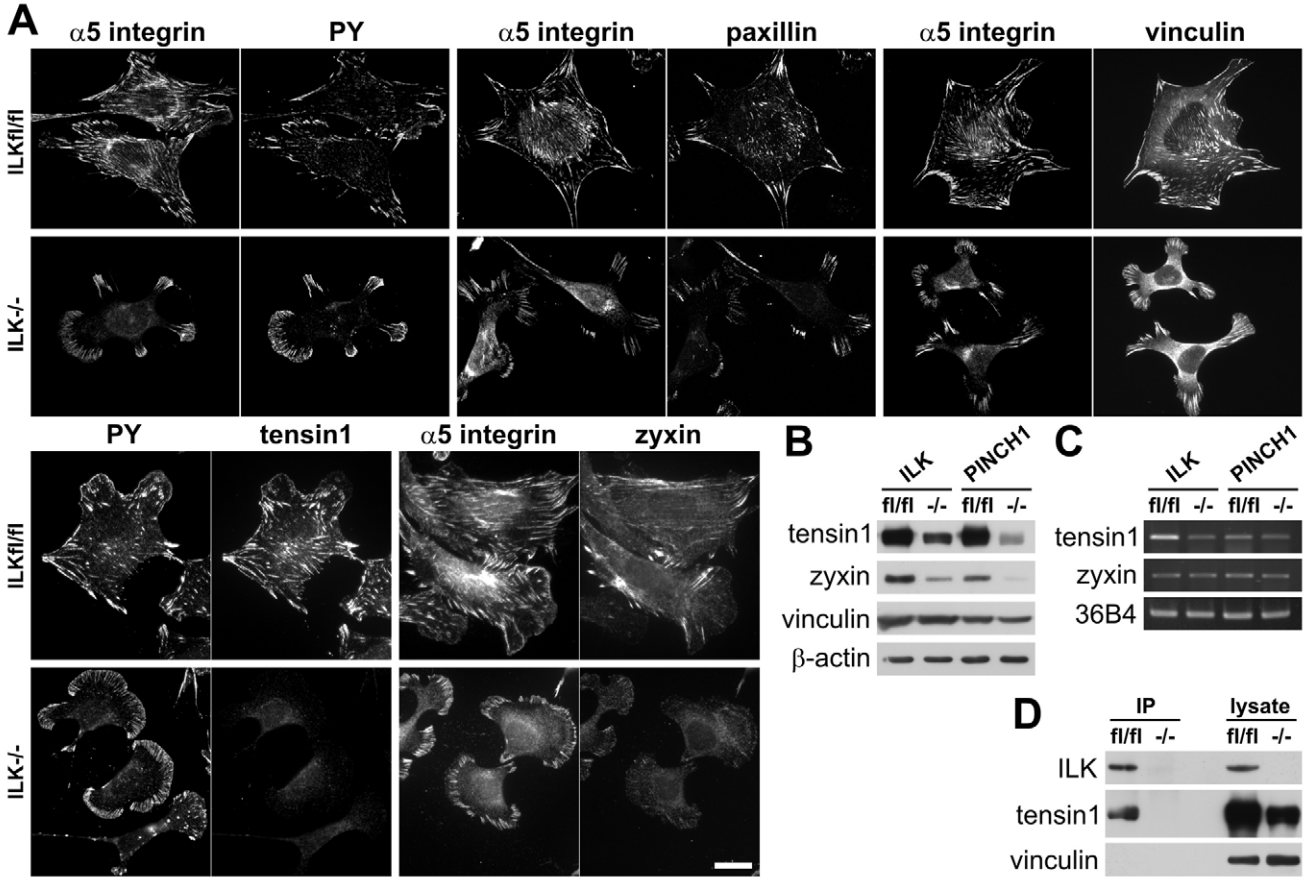

Fig. 1. Impaired adhesion maturation upon *ILK* or *PINCH1* deletion. (A) *ILK*$^{fl/fl}$ and *ILK*$^{-/-}$ cells plated on FN-coated coverslips and stained with antibodies against adhesion components. Scale bar: 20 μm. (B,C) Western blot of protein extracts (B) and RT-PCR on RNA extracts (C) from *ILK*$^{fl/fl}$, *ILK*$^{-/-}$, *PINCH1*$^{fl/fl}$ and *PINCH1*$^{-/-}$ cells. (D) Immunoprecipitation of endogenous ILK in extracts of *ILK*$^{fl/fl}$ and *ILK*$^{-/-}$ (negative control) cells.

Tensin has been implicated previously in FB formation (Pankov et al., 2000). Indeed, the downregulation of tensin1 observed in *ILK*- and *PINCH1*-null fibroblasts was accompanied by a lack of FBs. Not surprisingly, in the absence of these matrix-forming adhesions, we observed a major defect in FN fibrillogenesis, although no impact on FN secretion could be detected (supplementary material Fig. S1). We then sought to determine whether exogenous tensin could restore FA maturation in *ILK*- and *PINCH1*-null cells. To do so, a retrovirus encoding chicken tensin dually tagged with a Flag epitope and monomeric red fluorescent protein (mRFP) was transduced in $ILK^{fl/fl}$ and $PINCH1^{fl/fl}$ cells. Single clones expressing the transgene were isolated ($ILKT^{fl/fl}$, $PINCH1T^{fl/fl}$) and retroviral-mediated Cre recombination was performed to obtain $ILKT^{-/-}$ and $PINCH1T^{-/-}$ cells. Western blotting confirmed the expression of Flag-RFP-tensin, as well as the absence of ILK and PINCH1 proteins in $ILKT^{-/-}$ and $PINCH1T^{-/-}$ clones (Fig. 2A). In agreement with previous reports, *ILK* or *PINCH1* deletion was accompanied by a trans-downregulation of PINCH1 and ILK, respectively (Fukuda et al., 2003; Li et al., 2005; Stanchi et al., 2005).

In $ILKT^{fl/fl}$ and $PINCH1T^{fl/fl}$ cells, localization of Flag-RFP-tensin was identical to that of the endogenous protein (mostly in centrally positioned adhesions containing high levels of α5 integrin but low amounts of PY, morphologically similar to mature FAs or FBs) (Fig. 2B). By contrast, in $ILKT^{-/-}$ cells and $PINCH1T^{-/-}$ cells, Flag-RFP-tensin accumulated in perinuclear aggregated structures and it was only barely detectable in FAs. As described above, in the absence of ILK or PINCH1, α5 integrin remained in peripheral PY-rich adhesions without colocalizing with Flag-RFP-tensin (Fig. 2B, quantified in Fig. 2C), suggesting that tensin availability is not a limiting factor for adhesion maturation.

Collectively, these data suggest that *ILK* or *PINCH1* deletion, although permissive for FX and 'early' FA formation, abrogates their maturation to 'late' FAs and FBs, as defined by topology and recruitment of tensin and zyxin.

Tension destabilizes the adhesions of *ILK*- and *PINCH1*-null cells

Real-time analysis of cell shape changes provided important insights into the mechanisms underlying impaired FA maturation in the *ILK*- and *PINCH1*-null cells. Both $ILK^{-/-}$ and $PINCH1^{-/-}$ cells undergo cycles of rapid membrane retraction and frequent cell rounding. Thus, at any given time, between 20-30% of the cells in the population are round (Fig. 3B; supplementary material Movies 1-4), suggesting that the adhesion defect in *ILK*- and *PINCH1*-null cells might stem from reduced maintenance of cell-matrix contacts.

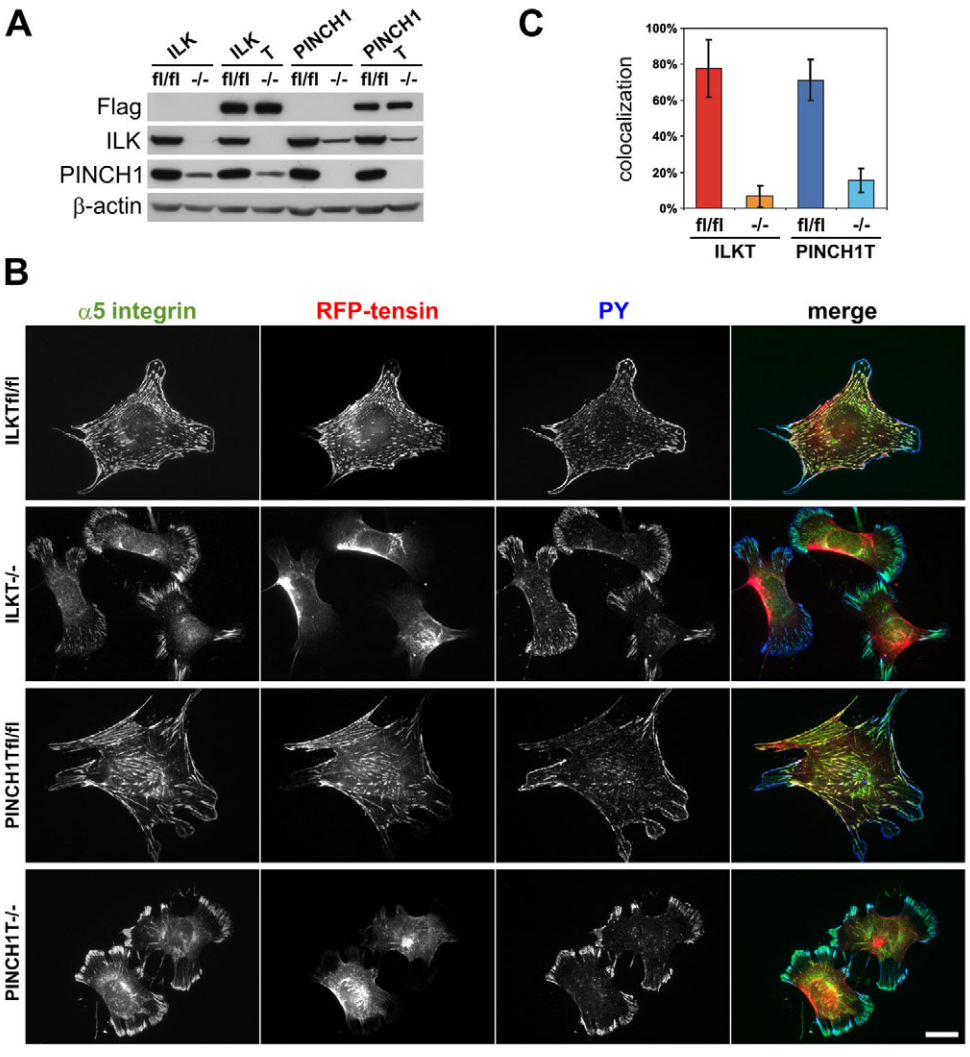

Fig. 2. Altered subcellular localization of tensin after *ILK* or *PINCH1* deletion. (A) Western blot analysis of ILK and PINCH1 cells and clones expressing Flag-RFP-tensin (ILKT and PINCH1T), detected using antibody against Flag. (B) Anti-integrin α5 and anti-PY staining of ILKT and PINCH1T cells on FN-coated coverslips. Scale bar: 20 μm. (C) Percentage of tensin colocalization with α5 integrin (±s.d., n=7) determined using the Metamorph colocalization function on images of single cells.

As previous work has shown that microtubule (MT) disruption with nocodazole stabilizes FAs (Kaverina et al., 1999), we tested whether FA stabilization by disruption of the MT network in *ILK*- and *PINCH1*-null cells would inhibit cell retraction. In control $ILK^{fl/fl}$ and $PINCH1^{fl/fl}$ cells, nocodazole-induced MT collapse was accompanied by an increase in cytoskeletal tension, clearly visible at 45 minutes by a change in cell morphology, an increase in FAs and a thickening of actin stress fibers (Fig. 3A; and F.S., unpublished results). In $ILK^{-/-}$ and $PINCH1^{-/-}$ cells, rather than reinforcing FAs, nocodazole significantly perturbed adhesion and cells rounded up within 2-10 minutes (Fig. 3B; supplementary material Movies 1 and 2).

Maturation of FAs under normal conditions and upon MT disruption is associated with increased cytoskeletal tension (Kirchner et al., 2003). To determine whether this underlies the sudden collapse of *ILK*- and *PINCH1*-null Fas, we treated cells with the ROCK inhibitor Y27632 to relax actomyosin-mediated contractility. ROCK inhibition had little effect on the spreading of $ILK^{fl/fl}$ and $PINCH1^{fl/fl}$ cells, whereas relieving endogenous force in $ILK^{-/-}$ and $PINCH1^{-/-}$ cells halted their frequent contractions and substantially reduced the number of round cells in the populations (Fig. 3B; supplementary material Movies 3 and 4).

To monitor the effect of endogenous cytoskeletal tension on tensin localization, we generated clones of $ILK^{fl/fl}$ and $PINCH1^{fl/fl}$ cells dually transduced with retroviruses encoding Flag-RFP-tensin and β-actin-GFP ($ILKTA^{fl/fl}$ and $PINCH1TA^{fl/fl}$). Subsequently, knockout clones were derived by Cre recombination ($ILKTA^{-/-}$ and $PINCH1TA^{-/-}$). As long-term fluorescence exposure was toxic to cells, we induced a rapid increase in cell contractility with nocodazole and filmed for short periods of time. Flag-RFP-tensin remained in stabilized FAs following drug treatment in the parental $ILKTA^{fl/fl}$ (Fig. 3C; supplementary material Movie 5) and $PINCH1TA^{fl/fl}$ cells (F.S., unpublished results). By sharp contrast,

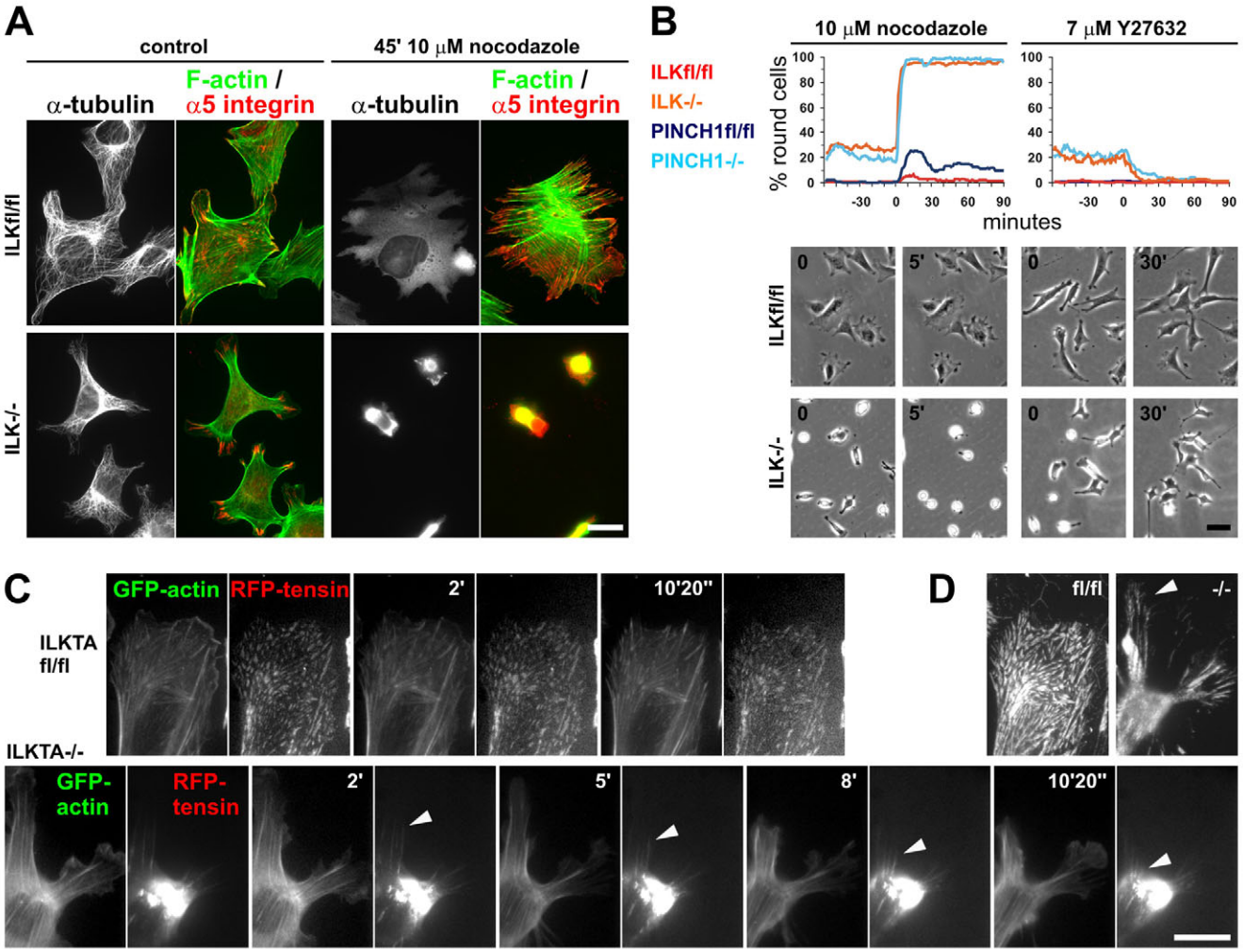

Fig. 3. Instability of *ILK*- and *PINCH*-null adhesions. (A) Phalloidin, anti-α-tubulin and anti-α5 integrin staining of cells plated on FN-coated glass coverslips and treated, or not treated, with 10 μM nocodazole for 45 minutes. Scale bar: 20 μm. (B) Time-lapse analysis of nocodazole and Y27632 treatment of ILK and PINCH1 cells. Cells plated on tissue culture dishes for 8 hours were filmed for 60 minutes before and 90 minutes after the addition of compounds (time 0), with frame rate (time interval between each frame) 1 minute. The percentage of round cells is indicated (mean of three different films, $n \geq 40$ cells/film). Extracts from the videos are available (supplementary material Movies 1-4); images from supplementary material Movies 1 and 3 correspond to the indicated times, in minutes (scale bar: 50 μm). (C,D) Time-lapse analysis of the effect of increased cytoskeletal tension on adhesions in $ILKTA^{fl/fl}$ and $ILKTA^{-/-}$ cells, plated on FN-coated coverslips and filmed immediately after the addition of 10 μM nocodazole (frame rate 20 seconds). The first frame on the left corresponds to the time of nocodazole addition and the relative time (‘, minutes; ‘’, seconds) is indicated in subsequent frames (C). Arrowheads indicate patches of RFP-tensin moving centripetally with F-actin. Scale bar: 20 μm. Complete videos are available (supplementary material Movies 5 and 6). (D) Anti-α5 staining on the same cells, fixed immediately after the time lapse.

addition of nocodazole to *ILKTA*$^{-/-}$ and *PINCH1TA*$^{-/-}$cells led to an abrupt retraction of actin stress fibers and centripetal movement of Flag-RFP-tensin. This retraction coincided with the perinuclear accumulation of Flag-RFP-tensin described above, suggesting that, after its initial localization in Fas, tensin is released from these structures together with F-actin (Fig. 3C, supplementary material Movie 6; and F.S., unpublished results). This was not attributable to overexpression of β-actin-GFP as phalloidin staining of *ILKT*$^{-/-}$ and *PINCHT*$^{-/-}$ cells also showed tensin aggregates colocalizing with short, speckled endogenous F-actin structures (F.S., unpublished results). Staining of cells fixed immediately after time-lapse analysis revealed that contracted *ILKTA*$^{-/-}$ and *PINCH1TA*$^{-/-}$ cells left substantial amounts of α5 integrin attached to the substrate (Fig. 3D, arrowhead; and F.S., unpublished results). Thus, in the absence of ILK or PINCH1, cytoskeletal tension disrupts the integrin–F-actin linkage, suggesting that ILK and PINCH might serve to relay endogenous force to adhesions as they mature.

Deletion of *ILK* or *PINCH1* impacts on the whole IPP complex

Gene ablation is a powerful strategy for dissecting signaling cascades and establishing the functional hierarchy among different proteins within a pathway, but in the case of the IPP complex this

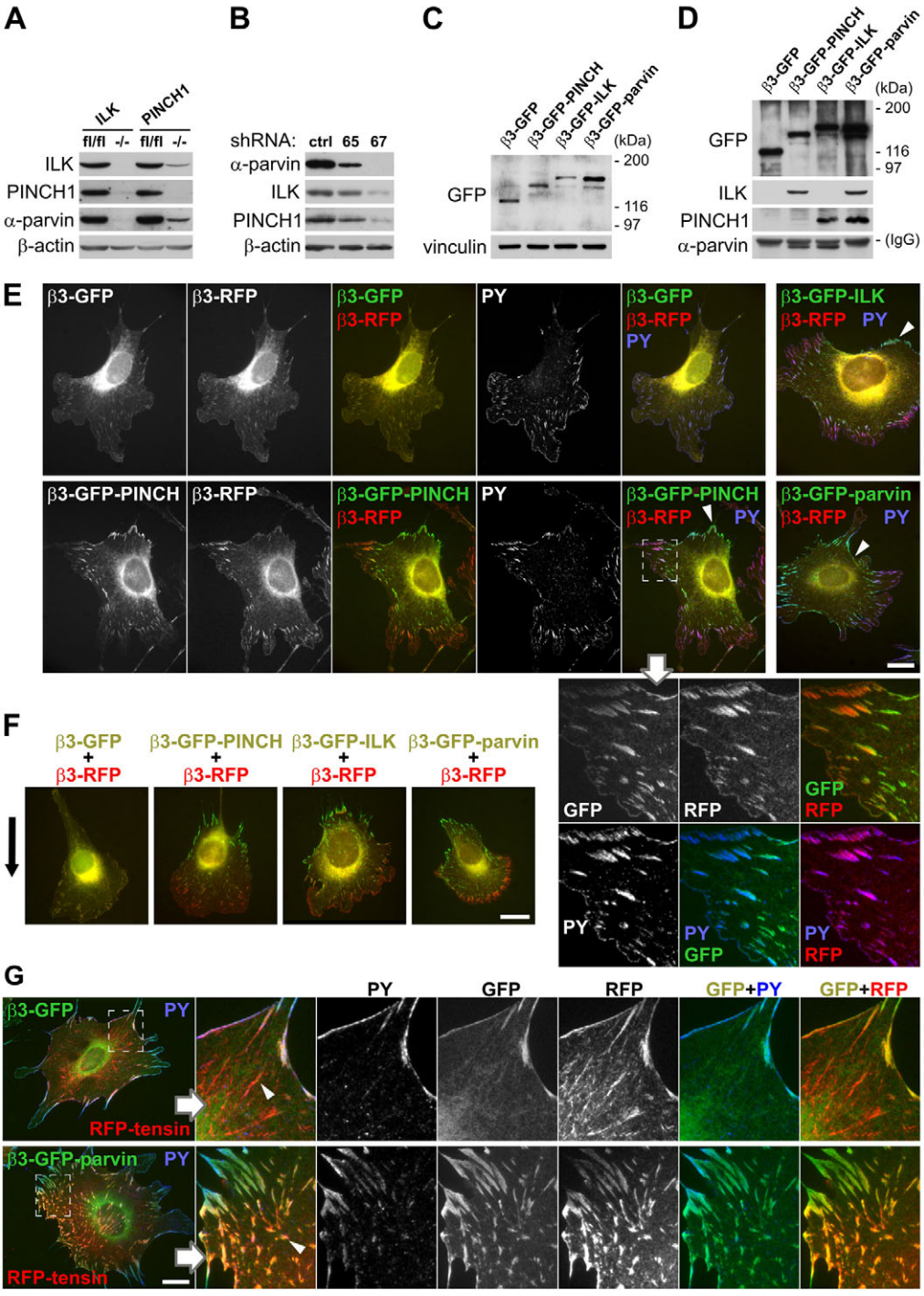

Fig. 4. Interdependency of the IPP components and constitutive targeting of the complex to β3 integrin. (A,B) Western analysis of ILK, PINCH1 and α-parvin levels in protein extracts from ILK and PINCH1 cells (A), or (B) *ILK*$^{fl/fl}$ cells stably infected with control or α-parvin-targeting shRNA lentiviruses (65 or 67). (C-F) Expression of integrin β3-GFP and β3-GFP-IPP chimeras in a clone of 3T3/β3-RFP cells. Western blotting on total lysates (C) and endogenous ILK, PINCH1 and α-parvin co-immunoprecipitation with the β3-GFP-IPP chimeras using an antibody against GFP (D). (E) Anti-PY staining. Arrowheads denote FAs in which each of the β3-GFP-IPP chimeras is recruited more efficiently than the co-expressed β3-RFP. (F) Differential distribution of each β3-GFP-IPP chimera with respect to the β3-RFP internal control in migrating cells. The black arrow indicates the presumed direction of migration, as deduced by cell morphology. (G) Staining of NIH3T3 cells expressing Flag-RFP-tensin together with β3-GFP (control) or β3-GFP-parvin. Arrowheads mark PY-poor and tensin-rich adhesions in which the β3-GFP-IPP chimera, but not the β3-GFP control, is enriched. Scale bars: 20 μm.

analysis is complicated by the interdependency of the component proteins for their stability and localization in integrin plaques (Fukuda et al., 2003; Li et al., 2005; Stanchi et al., 2005; Zhang et al., 2002). Accordingly, western blot analysis showed that deletion of *ILK* or *PINCH1* leads not only to the respective downregulation of PINCH1 or ILK proteins but also of α-parvin (Fig. 4A). Re-expression of GFP-tagged ILK in *PINCH1*$^{-/-}$ cells, or GFP-PINCH1 in *ILK*$^{-/-}$ cells, failed to restore a spread phenotype and FA targeting of the proteins (F.S., unpublished results), consistent with the notion that an intact ternary IPP is required for FA residence (Zhang et al., 2002). Therefore, the similar phenotype observed in *ILK*- and *PINCH1*-null cells presumably reflects the functional ablation of the entire complex. Not surprisingly, silencing of expression of α-parvin in *ILK*$^{fl/fl}$ fibroblasts by small hairpin RNA reduced the levels of ILK and PINCH1 proteins (Fig. 4B), impaired cell spreading and perturbed FA maturation, as determined by tensin1 and zyxin staining (D.G., unpublished results).

Constitutive targeting of the IPP complex to the β3 integrin subunit

To investigate further the role of the IPP complex in adhesion maturation and tensin recruitment, we employed a novel gain-of-function approach that involved targeting the IPP complex to a β integrin subunit by chimeric fusion. GFP-tagged β3 integrin was chosen for two reasons. First, for this strategy, we needed to use an integrin subunit that is normally enriched in PY-rich FXs and 'early' FAs, but not in PY-poor 'mature' FAs or FBs containing tensin (Zaidel-Bar et al., 2003). Second, this GFP-fusion has previously been shown to be fully functional (Ballestrem et al., 2001) and in fibroblasts it forms a single integrin heterodimer (αvβ3) that can be monitored by fluorescence microscopy. Thus, a set of retroviral constructs encoding ILK, PINCH1 or α-parvin fused to the cytoplasmic tail of β3-GFP was constructed. The cellular distribution of unmodified β3 integrin was followed using retroviral constructs encoding the β3 subunit tagged with GFP or mRFP.

To validate this approach, NIH3T3 cells with normal ILK and PINCH1 levels were transduced with the β3-RFP retrovirus, then a single clone was isolated (3T3/β3-RFP) and transduced with vector encoding β3-GFP or one of the 'β3-GFP-IPP chimeras' (β3-GFP-ILK, β3-GFP-PINCH, β3-GFP-parvin).

Western blot analysis using antibody against GFP showed bands of the expected sizes and similar intensities for each construct (Fig. 4C). Targeting of the entire IPP complex to each of the β3-GFP-IPP chimeras was verified by immunoprecipitation with antibody against GFP followed by western blotting to detect the presence of endogenous ILK, PINCH1 and α-parvin proteins. The endogenous proteins were undetectable in immunoprecipitates of integrin β3-GFP-expressing cells, whereas substantial amounts co-precipitated with their chimeric partners (Fig. 4D).

The distribution of the constructs was analyzed in cells plated on glass coverslips and stained with antibody against PY. In control cells, β3-GFP and β3-RFP colocalized completely, and substantial overlap was observed with PY staining, demonstrating that the fluorescent tags did not differentially affect localization of the integrin subunit (Fig. 4E). By contrast, addition of the IPP complex clearly altered its localization. Thus, the three β3-GFP-IPP chimeras were enriched in adhesions with weak PY staining that localized more centrally in the cells, or in what appeared to be retracting cell edges (Fig. 4E, arrowheads). Their accumulation in these older adhesions beneath the cell body and at the trailing edge of motile cells (Fig. 4F) suggests that they display a greater stability than adhesions formed by β3-RFP or β3-GFP. When expressed at slightly higher levels (as judged by fluorescence intensity), the β3-GFP-IPP chimeras, but not the β3-GFP control, completely replaced β3-RFP in all the adhesions (F.S., unpublished results).

We then assessed whether the re-deployment of β3-GFP following its fusion with IPP components coincided with the recruitment of tensin. To do this, β3-GFP and the β3-GFP-IPP chimeras were transduced in a clone of NIH3T3 cells expressing Flag-RFP-tensin. Flag-RFP-tensin colocalized poorly with β3-GFP/PY, whereas it was highly enriched in the PY-poor adhesions formed by the β3-GFP-IPP chimeras. Hence, fusion of PINCH1, ILK or α-parvin to the cytoplasmic tail of β3 integrin leads to its tight association with the entire IPP complex and prompts it to form tensin-rich PY-poor adhesions.

The IPP complex controls maturation of integrin adhesion

To determine whether the IPP-coupled integrins play a causal role in tensin recruitment and the maturation of late FAs, we expressed the β3-GFP-IPP chimeras, or the β3-GFP control, in *PINCH1T*$^{-/-}$ cells (see Fig. 2) that lack these structures. Western blot analysis revealed similar expression levels for each construct and, in some cases, a rescue of endogenous ILK or α-parvin (Fig. 5A). Thus, in the *PINCH1*-null background, expression of β3-GFP-PINCH restored ILK and α-parvin to control levels, expression of β3-GFP-ILK rescued α-parvin, and β3-GFP-parvin partially rescued ILK. The localization of the β3-GFP-IPP chimeras in *PINCH1T*$^{-/-}$ cells was analyzed in cells stained for several FA markers. Similar to the NIH3T3 cells described above, β3-GFP remained in peripheral PY-rich adhesions, without rescuing the defective recruitment of Flag-RFP-tensin (Fig. 5B). Conversely, expression of β3-GFP-PINCH prompted the abundant formation of small adhesions containing tensin distributed throughout the cell body. These structures could easily be distinguished from the perinuclear tensin aggregates observed in the *PINCH1T*$^{-/-}$ cells as they contained αv integrin and low, but detectable, amounts of PY, vinculin (Fig. 5B,C,E) and paxillin (F.S., unpublished results). However, they were devoid of α5 and β1 integrins (Fig. 5D; and F.S., unpublished results). Surprisingly, in this *PINCH1*-null background, both β3-GFP-ILK and β3-GFP-parvin chimeras exhibited an identical distribution and exerted similar effects on the localization of tensin (Fig. 5E), suggesting that PINCH1 might not be directly required for this function. Treatment of cells with two different αv antagonists (Maubant et al., 2006) had no effect on the normal tensin-rich adhesions of *PINCH1*$^{fl/fl}$ cells but dissolved the tensin-rich adhesions formed in *PINCH1*$^{-/-}$ cells by the β3-GFP-IPP chimeras, suggesting that they function as bona fide αvβ3 adhesion receptors (supplementary material Fig. S2). Thus, constitutive targeting of the IPP complex to β3 integrin selectively confers upon αvβ3 heterodimers the ability to mature tensin-rich adhesions in an IPP-null background.

Functional dissection of the ILK-PINCH-parvin complex

In an attempt to functionally dissect the IPP complex, we built a set of retroviral constructs encoding deletion mutants of the β3-GFP-IPP chimeras including two integrin β3-GFP-PINCH1 chimeras containing only the LIM1 domain (β3-GFP-LIM1) or lacking it (β3-GFP-ΔLIM1), two β3-GFP-ILK chimeras lacking the ankyrin repeat (β3-GFP-ΔAnk) or the kinase domain (β3-GFP-ΔKin) and two β3-GFP-α-parvin chimeras lacking the CH1 (β3-GFP-ΔCH1) or CH2 (β3-GFP-ΔCH2) domain. This new set of constructs was transduced in 3T3/β3-RFP cells, then protein

expression and the ability of the various IPP domains to associate with endogenous members of the IPP complex were determined by western blotting and co-immunoprecipitation (Fig. 6A,B). Fig. 6D schematizes the domains of PINCH1, ILK and α-parvin that mediate IPP complex interactions and the results of the co-immunoprecipitation assays. As expected, β3-GFP-LIM1, but not β3-GFP-ΔLIM1, co-immunoprecipitated endogenous ILK and α-parvin proteins; β3-GFP-ΔAnk and β3-GFP-ΔKin co-precipitated only α-parvin and only PINCH1, respectively; β3-GFP-ΔCH1, but not β3-GFP-ΔCH2, co-immunoprecipitated both endogenous ILK and PINCH1.

The ability of the various IPP domains to drive adhesion maturation, as assessed by displacement of β3-GFP-containing adhesions with respect to control β3-RFP-tagged adhesions, was quantified by analyzing 16-bit grayscale-ratio images obtained by dividing GFP by RFP images of single cells. Identical distribution of GFP and RFP-tagged constructs yields a constant GFP:RFP ratio in all the FAs of a given cell (visualized as uniform gray intensity), whereas a different distribution leads to local variations of the ratio (and non-uniform gray intensity). Metamorph software was used to analyze the intensity standard deviation (i.s.d.) values on a set of ratio images of single cells from each population (supplementary material Fig. S3). Images from control cells expressing β3-GFP gave low i.s.d. values, in the range of the background noise of the detection system. Conversely, i.s.d. values were significantly higher in images from cells expressing the full-length β3-GFP-IPP chimeras, reflecting their differential distribution with respect to the β3-RFP internal control (Fig. 6C). In the case of the deletion mutants, high i.s.d. values were obtained for β3-GFP-LIM1, β3-GFP-ΔAnk and β3-GFP-ΔCH1 chimeras, whereas low i.s.d. values were observed for β3-GFP-ΔLIM1, β3-GFP-ΔKin and β3-GFP-ΔCH2 chimeras. The same pattern for tensin recruitment to the chimeric integrins was observed, using a clone of NIH3T3 cells expressing Flag-RFP-tensin (F.S., unpublished results).

Combined, these observations indicate that a defined region of the IPP complex, comprising the C-terminal domain of ILK and/or the CH2 domain of α-parvin, represents the minimal functional unit required for tensin recruitment and integrin redistribution. Either fused directly to β3-GFP or recruited through interaction with other fused IPP components, these domains are associated with all the integrin β3 chimeric constructs that exhibit a shift in localization, whereas they are absent in all of those that did not (Fig. 6D).

The IPP components stabilize each other through a binding-dependent mechanism

To extend these observations, β3-GFP-IPP deletion mutants were expressed in *PINCHT*$^{-/-}$ and *ILKT*$^{-/-}$ cells. First, we examined the integrity of the IPP complex (i.e. stability of the IPP components) in the different cells by western blotting. Results from these analyses are shown in the top of Fig. 7, and schematic representations of the IPP components present in each cell line and their resulting interactions are pictured below. Thus, expression of the ILK-binding β3-GFP-LIM1 PINCH1 chimera in *PINCH1*$^{-/-}$ cells restored endogenous ILK levels, whereas β3-GFP-ΔLIM1 did not. The ILK-binding β3-GFP-ΔCH1 α-parvin chimera showed a similar effect, albeit more moderate, whereas the β3-GFP-ΔCH2 chimera did not. In both *PINCH1*- and *ILK*-null cells, the α-parvin-binding kinase domain of ILK (β3-GFP-ΔAnk chimera), but not the N-terminal ankyrin repeat region (β3-GFP-ΔKin chimera),

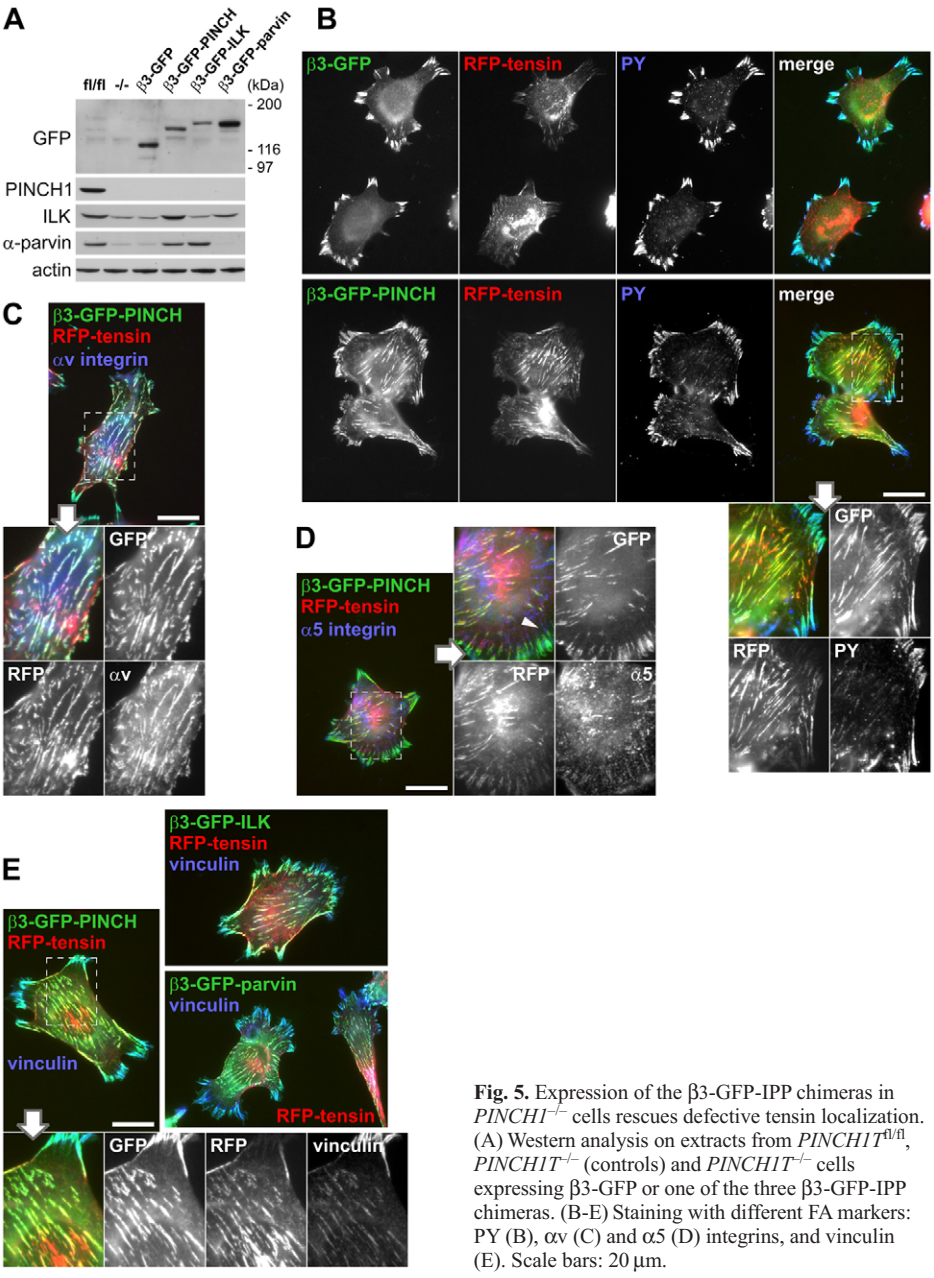

Fig. 5. Expression of the β3-GFP-IPP chimeras in *PINCH1*$^{-/-}$ cells rescues defective tensin localization. (A) Western analysis on extracts from *PINCH1T*$^{fl/fl}$, *PINCH1T*$^{-/-}$ (controls) and *PINCH1T*$^{-/-}$ cells expressing β3-GFP or one of the three β3-GFP-IPP chimeras. (B-E) Staining with different FA markers: PY (B), αv (C) and α5 (D) integrins, and vinculin (E). Scale bars: 20 μm.

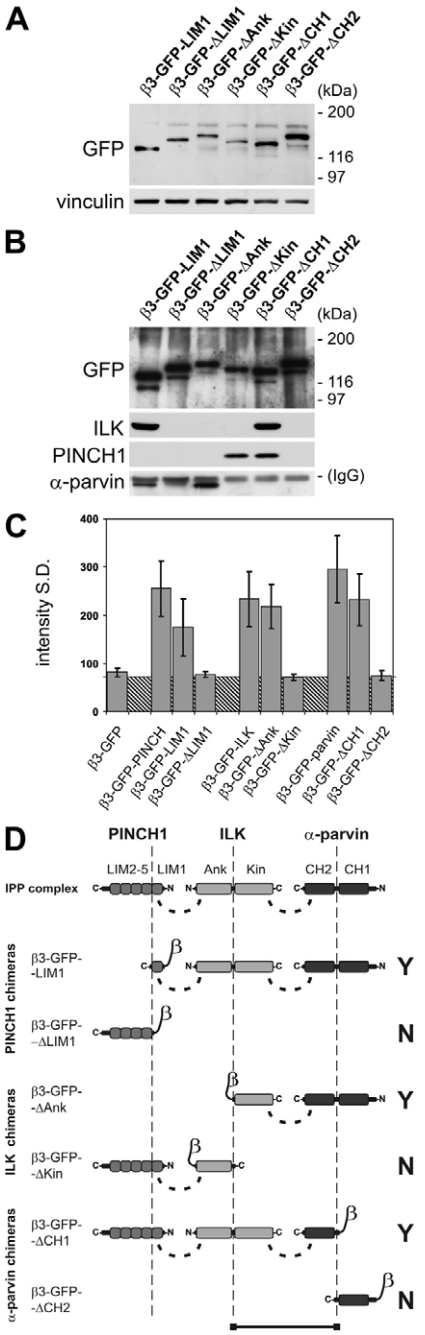

Fig. 6. Dissection of the IPP complex function by expression of deletion mutants of the β3-GFP-IPP chimeras in a clone of 3T3/β3-RFP cells. (A) Detection of the expressed constructs by western blots on total lysates. (B) Co-immunoprecipitation of the chimeric proteins with an antibody against GFP and detection of endogenous IPP complex proteins in the co-precipitate. (C) Differential localization of all β3-GFP-IPP chimeras with respect to β3-RFP. Average i.s.d. values (s.d.) obtained by processing GFP:RFP ratio images of 12 cells from each population, as described in supplementary material Fig. S3. The dashed area indicates the system background noise i.s.d. (D) Combined results of co-immunoprecipitation and fluorescence ratio image analysis. Different protein domains in PINCH1, ILK and α-parvin proteins and their interactions (bold broken lines) are represented (Ank, ankyrin repeat; Kin, kinase domain). 'β' indicates sites of fusion of integrin β3-GFP with each deletion mutant; co-immunoprecipitated proteins of the IPP complex are indicated. The differential localization of constructs (as compared with the internal control β3-RFP) determined in the ratio image analysis is indicated (Y, yes; N, no). The bar below specifies the 'region' within the IPP complex endowed with this ability.

rescued endogenous α-parvin levels, whereas expression of the PINCH1-binding ILK ankyrin repeats (β3-GFP-ΔKin chimera) rescued PINCH1 levels in *ILK*$^{-/-}$ cells. Finally, β3-GFP-LIM1 caused an increase in endogenous α-parvin protein in *PINCH1*$^{-/-}$ but not in *ILK*$^{-/-}$ cells, indicating that its effect on α-parvin protein stability is due to the rescue of endogenous ILK (schematized in Fig. 7).

Together with our co-immunoprecipitation data above, these observations show that stability of the ILK, PINCH1 and α-parvin proteins is intimately linked to their direct interaction.

Integrin targeting of the ILK kinase domain is required for the FA maturation

Next, the effect of the β3-GFP-IPP deletion mutants on tensin localization was examined in *PINCH1T*$^{-/-}$ and *ILKT*$^{-/-}$ cells. Consistent with our observations in NIH3T3 cells, only the deletion mutants β3-GFP-LIM1, β3-GFP-ΔAnk and β3-GFP-ΔCH1 retained the ability to form tensin-rich FAs in *PINCH1T*$^{-/-}$ cells (supplementary material Fig. S4A).

In the *ILKT*$^{-/-}$ cells, only the β3-GFP-ΔAnk chimera prompted the formation of tensin-rich adhesions, whereas all the other constructs, including β3-GFP-LIM1 and β3-GFP-ΔCH1, did not (supplementary material Fig. S4B). Similarly, the full-length β3-GFP-PINCH and β3-GFP-parvin chimeras did not rescue FA recruitment of tensin in *ILKT*$^{-/-}$ cells (F.S., unpublished results and Fig. 8F), indicating that targeting the ILK kinase domain to integrins is strictly required for this event. Interestingly, *ILKT*$^{-/-}$ cells expressing β3-GFP-ΔAnk showed increased spreading (Fig. 8A), which was not observed in *ILKT*$^{-/-}$ cells expressing the other constructs.

Besides interacting with members of the parvin protein family, the ILK C-terminal domain interacts with paxillin (Nikolopoulos and Turner, 2002) and has been reported to possess Ser/Thr kinase activity (Hannigan et al., 1996). We next introduced point mutations in the β3-GFP-ΔAnk chimera that have previously been shown to impair these functions. The first mutation, V386G-T387G was shown to abrogate the paxillin-binding site (PBS) of ILK (Nikolopoulos and Turner, 2002) and the second, K220G, ablates a lysine residue in the ILK ATP-binding site reportedly essential for kinase activity (Yamaji et al., 2001).

Similar to the β3-GFP-ΔAnk construct, expression of the PBS mutant in *ILKT*$^{-/-}$ cells increased cell spreading, albeit to a lesser extent than the wild-type construct, whereas the K220G mutant was not competent for this effect (Fig. 8A). Interestingly, both the effect on cell spreading and on the ability to prompt the formation of tensin-rich adhesions correlated with the capacity of the mutant constructs to bind to α-parvin, observed in co-immunoprecipitation experiments, suggesting that α-parvin is required for ILK-dependent FA maturation (Fig. 8B,C).

To test this, α-parvin was abrogated by small hairpin RNA knockdown in *ILKT*$^{-/-}$ cells expressing the β3-GFP-ΔAnk construct (Fig. 8D). Following α-parvin depletion, β3-GFP-ΔAnk remained in peripheral adhesions and no longer rescued the defective recruitment of Flag-RFP-tensin (Fig. 8E). As mentioned above, the expression of β3-GFP-parvin did not rescue adhesion maturation (Fig. 8F). Combined, these observations point to a requirement for both ILK and α-parvin for this effect.

With respect to paxillin binding, no paxillin was detectable in the co-immunoprecipitates of either wild-type or mutant constructs, suggesting that the interaction of the ILK kinase domain with paxillin might be weaker than its interaction with α-parvin. Indeed,

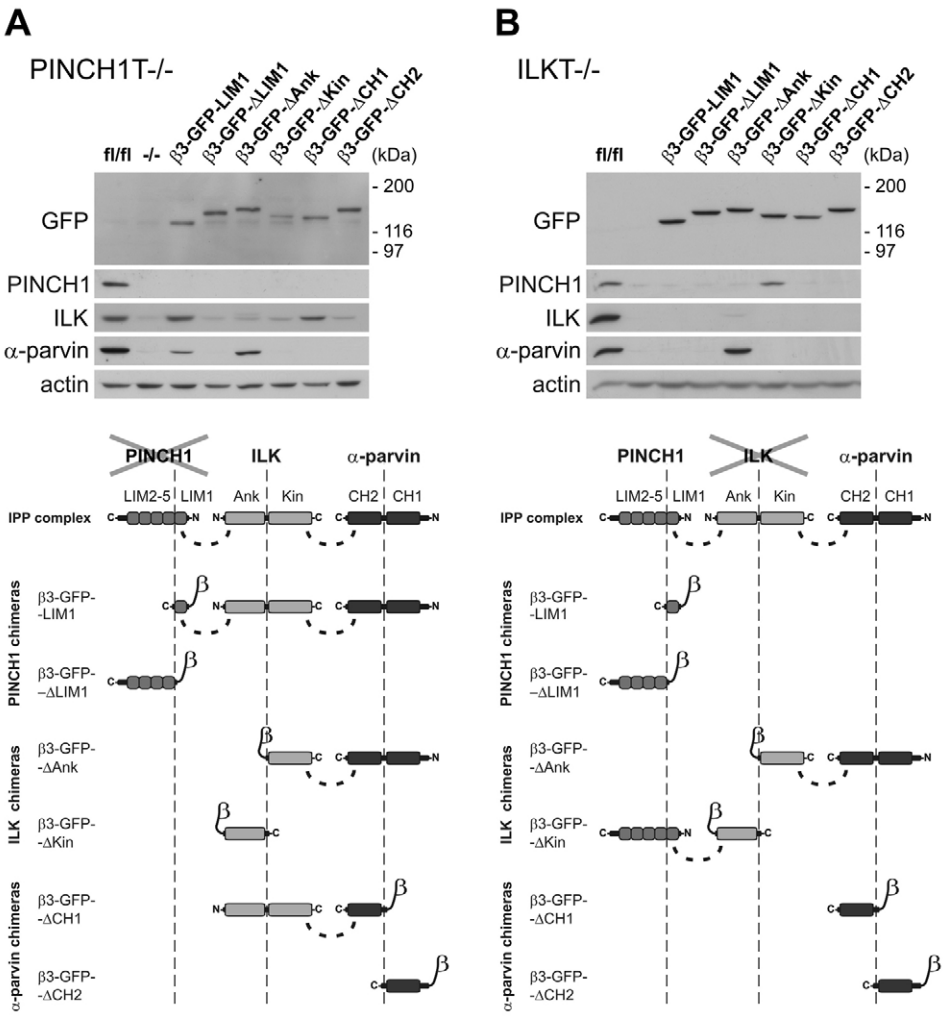

Fig. 7. Stabilization of IPP components depends on their direct interaction. Western blot analysis on lysates of *PINCH1T*$^{-/-}$ (A) or *ILKT*$^{-/-}$ cells (B) expressing the set of β3-GFP-IPP deletion mutants. Schematics below show the interactions between the chimeric proteins and endogenous IPP components that lead to their stabilization in the *PINCH1*-null and *ILK*-null backgrounds, respectively.

paxillin was detectable in the adhesions of all the cells, including the tensin-rich adhesions induced by expression of the PBS mutant, indicating that its localization does not depend upon direct binding to ILK (F.S., unpublished results).

Discussion

Here, we sought to investigate the role of ILK, PINCH1 and α-parvin in regulation of integrin-based adhesions using unique cellular models and chimeric proteins designed to dissect their function. Previous studies have documented the presence of the early FA components paxillin and vinculin in adhesions of *ILK*- and *PINCH1*-knockout cells (Sakai et al., 2003; Stanchi et al., 2005). We extended this work to include analysis of 'late' FA components, including tensin1, an F-actin capping and binding protein (Lo et al., 1994) and zyxin, a LIM-domain mechanosensitive protein (Yoshigi et al., 2005). Our results show that ablation of the IPP complex, by ILK or PINCH1 deletion, impacts on the recruitment of both tensin1 and zyxin to FAs, establishing these proteins as downstream targets of the IPP complex. Intriguingly, in *ILK*- and *PINCH1*-null cells, both tensin1 and zyxin proteins are downregulated by mechanisms that remain to be determined and that, in the case of tensin1, include a decrease in mRNA levels.

By virtue of its actin-binding activity, tensin has been proposed to be an important regulator of adhesion dynamics. Indeed, negative regulation by tensin of actin assembly by capping the barbed end of filaments (Chuang et al., 1995) could provide a mechanism to regulate the transmission of force between the actin cytoskeleton and FAs. However, restoring tensin expression alone in *ILK*- and *PINCH1*-deficient cells was not sufficient to drive FA maturation. As our study revealed, escalating force at the cytoskeletal membrane interface in *ILK*$^{-/-}$ and *PINCH1*$^{-/-}$ cells leads to a disruption of the integrin–F-actin linkage, even in presence of ectopically expressed tensin (Flag-RFP-tensin). In light of these findings, together with the established requirement for actomyosin-generated tension during FA formation or maintenance and integrin translocation (Pankov et al., 2000; Zamir et al., 1999; Zamir et al., 2000), we propose that the failure of IPP-null adhesions to sustain endogenous tension might explain their inability to support FA maturation and tensin recruitment. Colocalization between ILK and tensin might result from 'activation' of the IPP complex by an unknown mechanism, possibly involving α-parvin and F-actin. This finding would support the 'conformational switch' model of force-induced focal contact growth proposed by Geiger and Bershadski (Geiger and Bershadsky, 2001), in which force applied to specific adhesion-associated molecules might induce their conformational activation.

The novel strategy of imposed integrin localization of the IPP components used here allowed us: (1) to overcome the interdependency of the IPP proteins for their integrin association; (2) to assess the effects of IPP targeting to a specific integrin; and

(3) to evaluate the functional contribution of individual IPP components to adhesion maturation. We found that, in contrast to β3-GFP alone, fusion of β3-GFP with ILK, PINCH1 or α-parvin confers these chimeras with the ability to reconstitute the entire IPP triad at their cytoplasmic tails. The resulting IPP-bound αvβ3 dimers form adhesions that resemble mature FAs (as defined by their morphology, localization and relative abundance of tensin), both in NIH3T3 fibroblasts, expressing the complete set of endogenous IPP components, and in *ILK*- and *PINCH1*-null cells. Systematic analysis of motifs within the IPP complex (β3-GFP-IPP deletion mutants) for their ability to drive the formation of these mature FA structures allowed us to identify the ILK kinase domain as a key requirement for this function.

An important finding using this strategy is that the IPP complex, through the ILK kinase domain, can selectively control the organization of adhesive complexes and the dynamics of the integrin to which it associates. Thus, although the β3-GFP-IPP chimeras can form tensin-rich FAs in *PINCH1*$^{-/-}$ cells, their expression in this *PINCH1*-deficient background does not rescue the defective formation of these adhesions by α5β1 or by other β1 heterodimers that are unable to reconstitute the ternary complex. In light of our results here, and our previous findings that endogenous ILK colocalizes with the α5 integrin subunit (Vouret-Craviari et al., 2004), we propose that the process by which IPP binding to ligand-engaged α5β1 integrin prompts tensin recruitment and linkage to the actin cytoskeleton might underlie the α5β1 integrin segregation during FA maturation and FB formation. Concerning FB formation and FN assembly, the molecular mechanisms that regulate the binding of IPP to α5β1 are largely unknown. It has been shown using monoclonal antibodies that stepwise conformational changes in α5β1 integrin are associated with the process of FB formation and FN fibrillogenesis (Clark et al., 2005). We speculate that these changes, accompanied by ligand occupancy, might be linked to transitional events involving IPP association. It is noteworthy that, in our system, expression of the β3-GFP-IPP chimeras failed to drive complete FB maturation and FN fibrillogenesis (F.S., unpublished results) probably owing to intrinsic differences in FN binding activity of αvβ3 and α5β1 integrin, differences in their associated cytoplasmic protein complexes and/or co-receptors.

Current knowledge together with our present results suggests that recruitment of the IPP complex to integrins is subject to tight regulation that occurs at multiple levels. A first step involves the regulation of IPP complex formation. A second regulatory mechanism relies on proteasome-mediated degradation of the IPP components (Fukuda et al., 2003), which, as shown here, is intimately linked to the direct interaction between ILK, PINCH1 and α-parvin. Degradation of unbound IPP members could represent a 'check-point' for control of dominant-negative effects of accumulating 'incomplete' IPP complexes. Once a complete IPP complex has formed, a third level of regulation involves the establishment of parallel interactions between IPP components and other network proteins. The novel finding of our study that tensin and zyxin levels are sensitive to IPP components adds another layer of complexity to the tight control of adhesion dynamics.

The kinase domain of ILK was identified here as a key functional motif of the IPP complex; however, differences between signaling and structural or scaffolding functions of ILK are difficult to distinguish. Indeed, ILK kinase activity has been documented in numerous studies (reviewed by Legate et al., 2006). Nonetheless, the absence of the catalytic HRD and DFG motifs and the ability of a kinase-dead ILK to rescue *ILK*-null flies and worms have led to the classification of ILK as a pseudokinase with a scaffolding role (Boudeau et al., 2006; Legate et al., 2006). In our study, mutations in the ILK kinase domain of the β3-GFP-ΔAnk chimera ablating either paxillin (V386G-T387G) or ATP (K220G) binding impacted to varying degrees on its ability to rescue adhesion maturation. Mutations at these sites have previously been characterized in other systems, yet interpretation of their effects in terms of signaling has been complicated by their collateral impact on the

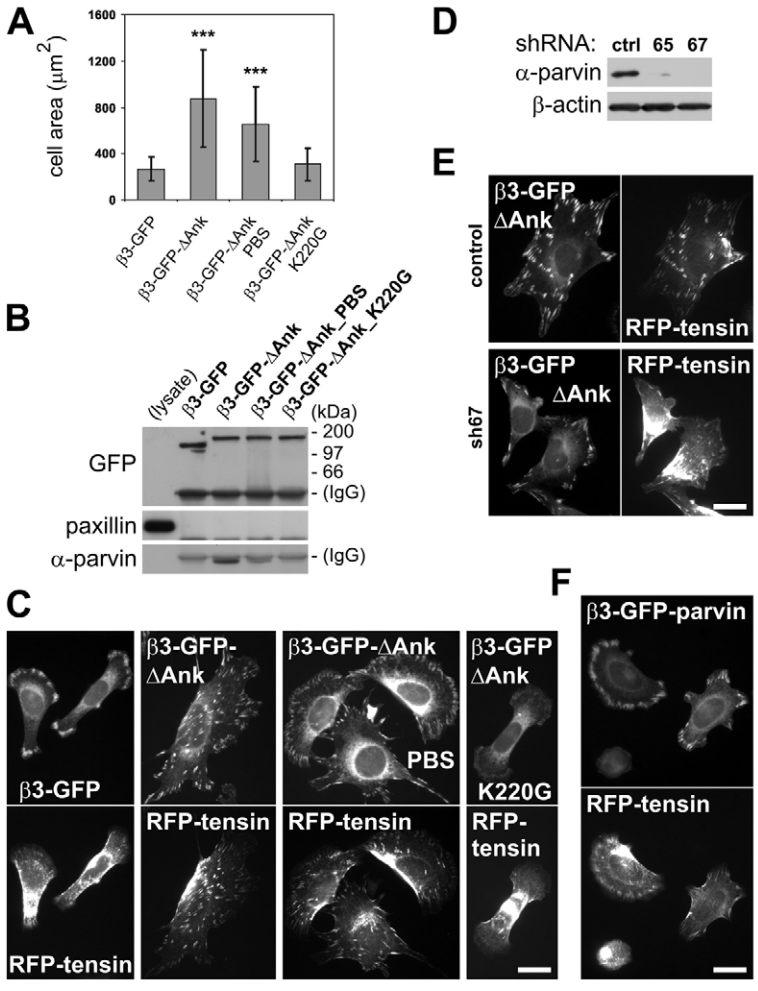

Fig. 8. Adhesion targeting of ILK kinase domain mutants in *ILK*$^{-/-}$ cells and effects of α-parvin silencing in *ILKT*$^{-/-}$ cells expressing β3-GFP-ΔAnk. (A) Quantification of spreading as compared with β3-GFP control cells ($n \geq 150$; ***$P<0.001$). (B) Co-immunoprecipitation of the constructs with antibody against GFP and detection of paxillin and α-parvin by western blotting. (C) Localization of the chimeric constructs and tensin. (D,E) *ILKT*$^{-/-}$ cells expressing β3-GFP-ΔAnk were stably infected with control or α-parvin-targeting shRNA lentiviruses (65 and 67), then analyzed by western blot (D) and stained as above (E). (F) *ILKT*$^{-/-}$ cells expressing β3-GFP-parvin plated on coverslips. Scale bars: 20 μm.

FA targeting of ILK and, probably, of the whole IPP complex (Nikolopoulos and Turner, 2002). In the present study, this problem has been circumvented by chimeric fusion with β3-GFP to ensure FA localization.

Turning to the role of paxillin, its phosphorylation on two tyrosine residues (Y31 and Y118) was shown to control integrin adhesion dynamics by regulating recruitment of focal adhesion kinase (FAK) (Zaidel-Bar et al., 2007). As the kinase domain of ILK binds to the first leucine-rich domain (LD) of paxillin (Nikolopoulos and Turner, 2001) – that is, near Y31 – it could participate in this paxillin-dependent control of adhesion dynamics. To date, the consequence of paxillin phosphorylation on ILK binding is not known. However, our results herein that a partial rescue of the $ILK^{-/-}$ phenotype occurred in cells expressing the PBS mutant (V386G-T387G) would argue that the observed effects of the ILK kinase domain do not depend exclusively upon direct interaction with paxillin. Indeed, although paxillin silencing in $ILK^{fl/fl}$ cells abrogates the FA localization of FAK and fibronectin fibrillogenesis, this defect can be rescued with an ILK-binding paxillin mutant, further indicating that the direct interaction between ILK and paxillin is not essential (C.G., unpublished results). Alternatively, paxillin phosphorylation could regulate adhesion dynamics by controlling FAK and IPP recruitment in parallel. It is noteworthy that the CH2 domain of α-parvin can also bind to paxillin, and recent structural evidence indicates that paxillin LD1 might bind simultaneously to ILK and α-parvin, forming a three-way ternary complex (Wang et al., 2008).

With regards to the catalytic function of ILK, our findings that the ATP-binding-deficient mutant (K220G) did not co-precipitate α-parvin from cell lysates, together with the fact that α-parvin silencing abrogated the observed effects of the ILK C-terminus, indicate that recruitment of this actin-binding partner is essential for the adhesion maturation function of ILK.

Studies in invertebrates first suggested that ILK might behave as an adaptor that links integrins to the actin cytoskeleton (Mackinnon et al., 2002; Zervas et al., 2001). Our results suggest that, in vertebrates, ILK might control FA maturation in a similar way by creating a 'docking platform' that connects F-actin through α-parvin with other actin-binding FA proteins, thereby reinforcing integrin-cytoskeleton linkage. Possible candidates for this co-operation include vinculin or filamin, which can be indirectly associated with ILK by their respective binding to paxillin or MIG2/kindlin-2 and migfilin (reviewed by Legate et al., 2006). As opposed to these early FA components, tensin is a relatively late addition to FAs with multiple actin-binding sites that has previously been shown to promote FB formation and FN assembly (Lo et al., 1994; Pankov et al., 2000). To date, our investigation is the first to establish a functional relationship between tensin and ILK in vertebrate cells, although similar findings in an invertebrate model suggest that this connection is conserved through evolution (Torgler et al., 2004). Similar to *ILK*- and *PINCH1*-null fibroblasts, both ILK and tensin *Drosophila* mutants display phenotypes that suggest a defect in the stabilization, but not in the initial formation of, integrin adhesions (Torgler et al., 2004; Zervas et al., 2001). Such conservation across evolution and complexity of regulation highlights the essential role of the IPP complex in integrin-dependent functions.

Materials and Methods

Retroviral constructs

Retroviral expression constructs encoding integrin β3-GFP, integrin β3-RFP and the IPP fusions were derived from a β3-GFP construct (Ballestrem et al., 2001). Flag-RFP-tagged tensin was derived from a construct for transient expression of GFP-tagged chicken tensin (Zamir et al., 2000). Mutagenesis was performed using the QuikChange II site-directed mutagenesis kit (Stratagene). All constructs were subcloned in the retroviral expression vector pCLMFG (Naviaux et al., 1996).

Cell culture

All cells were cultured in DMEM supplemented with 10% fetal bovine serum for ILK mouse kidney fibroblasts (Sakai et al., 2003), PINCH1 mouse embryonic fibroblasts (Stanchi et al., 2005) and Phoenix ecotropic cells (ATCC SD-3444), and 10% bovine serum for NIH3T3 cells.

Production of retroviruses

Phoenix ecotropic cells were transfected using the calcium phosphate method. Supernatants containing the retroviruses collected 48 and 60 hours post-transfection were supplemented with 5 μg/ml polybrene (Sigma) for infection of mouse fibroblasts.

RNA silencing

Small hairpin lentiviral plasmids from Sigma (MISSION shRNA clones TRCN0000112665-69) were used for stable silencing of RNA encoding α-parvin. Viral particles were produced in 293 cells by transient co-transfection with the silencing vector (pLKO.1-puro backbone), the virion packaging system p8.91 (Didier Trono, EPFL Lausanne, Switzerland) and the envelope plasmid pMD2.G (Addgene plasmid 12259, Addgene, Cambridge, MA) generated in the laboratory of D. Trono.

Cre-mediated gene deletion

Cre recombination was performed by infecting $ILK^{fl/fl}$ and $PINCH1^{fl/fl}$ fibroblasts with a self-excising Cre retrovirus (Silver and Livingston, 2001), prepared as described above. Cells were cloned and screened by PCR for gene deletion (Sakai et al., 2003; Stanchi et al., 2005).

RNA isolation and RT-PCR

Total RNA was isolated from cells using the Trizol reagent from Invitrogen. Semi-quantitative reverse-transcriptase polymerase chain reaction (RT-PCR) was performed using the OneStep RT-PCR kit from Qiagen. Amplification of 36B4 mRNA (GenBank accession number M17885) served as internal control. Forward and reverse primers used were, respectively, 5′-CGCCCCTGCTAAGCTCTTT-3′ with 5′-TCCATCCA-TACAGGGGATTC-3′ for tensin1 and 5′-CAGTGCTTCACCTGTGTGGT-3′ with 5′-CTGTGGTCTGGAAGGAGGTC-3′ for zyxin.

Materials and antibodies

Reagents, unless specified, were from Sigma. Tissue-culture plasticware was from Nunc. The primary antibodies used have been described previously (Chu et al., 2006; Li et al., 2005; Stanchi et al., 2005; Vouret-Craviari et al., 2004), except anti-β-actin mAbcam 8226 (Abcam), anti-phosphotyrosine clone 4G10 (Upstate Biotechnology), anti-tensin1 (kindly provided by Su Hao Lo, University of California Davis, CA), anti-zyxin clone B-5-1-2 (Synaptic Systems, Göttingen, Germany), anti-α-tubulin clone 164D4 (Zymed), anti-integrin αv (Chemicon). Antibodies conjugated to Alexa488, Alexa546 and Alexa647 were from Molecular Probes, and HRP-conjugated antibodies were from Promega.

Co-immunoprecipitation and western blotting

Immunoprecipitation, preparation of cell lysates, protein quantification and western blotting were performed as described previously (Stanchi et al., 2005), with the exception of anti-ILK immunoprecipitation, which was performed on cells lysed in NP40 lysis buffer (25 mM HEPES, 150 mM NaCl, 1 mM EGTA, 10 mM sodium pyrophosphate, 10 mM NaF, 5 mM sodium orthovanadate, 5 μg/ml leupeptin, 0.15 μM aprotinin, 1 mM AEBSF, complete, mini, EDTA-free; protease inhibitor cocktail tablet (Roche Diagnostics), 10% glycerol, 0.5% NP40) following brief sonication.

Immunofluorescence

Cells were plated on glass coverslips uncoated or, when specified, coated with 10 μg/ml FN, fixed after 4 hours and stained as described previously (Vouret-Craviari et al., 2004).

Microscopy

Samples were observed through 63× (1.4 NA) oil or 10× (0.25 NA) air objectives on an Axiovert 200M inverted microscope (Carl Zeiss) equipped with an incubator chamber and a CoolSnap HQ cooled charge-coupled-device camera (Roper Scientific, Evry, France); all images were acquired and analyzed using MetaMorph Imaging System (Universal Imaging).

We kindly acknowledge Bernhard Wehrle-Haller (Centre Médical Universitaire, University of Geneva, Switzerland), Benny Geiger (Weizmann Institute of Science, Rehovot, Israel) and Shokat Dedhar (British Columbia Cancer Research Centre of the BC Cancer Agency, Vancouver, BC, Canada) for providing cDNA constructs. The ILK

K220G mutant was generated by Etienne Boulter (University of Nice-Sophia Antipolis, Nice, France). We are indebted to Jérémy Thiblet (Roper Scientific, Evry) and Sébastien Schaub (PRISM Platform, UMR6543 CNRS/UNS/IBDC) for assistance with image analysis, and Nathalie Fratini (Polytechnique Universitaire de Nice-Sophia Antipolis, Sophia-Antipolis, France) for help during the early phase of these studies. This work was supported by the CNRS, the University of Nice-Sophia Antipolis (UMR6543), the Centre A. Lacassagne and the Max-Planck Society. E.V.O.-S. is an INSERM investigator. The Association pour la Recherche contre le Cancer (ARC), Canceropole PACA and the Emerald Foundation are gratefully acknowledged for additional support.

References

Ballestrem, C., Hinz, B., Imhof, B. A. and Wehrle-Haller, B. (2001). Marching at the front and dragging behind: differential alphaVbeta3-integrin turnover regulates focal adhesion behavior. *J. Cell Biol.* **155**, 1319-1332.

Boudeau, J., Miranda-Saavedra, D., Barton, G. J. and Alessi, D. R. (2006). Emerging roles of pseudokinases. *Trends Cell Biol.* **16**, 443-452.

Boulter, E., Grall, D., Cagnol, S. and Van Obberghen-Schilling, E. (2006). Regulation of cell-matrix adhesion dynamics and Rac-1 by integrin linked kinase. *FASEB J.* **20**, 1489-1491.

Chiswell, B. P., Zhang, R., Murphy, J. W., Boggon, T. J. and Calderwood, D. A. (2008). The structural basis of integrin-linked kinase-PINCH interactions. *Proc. Natl. Acad. Sci. USA* **105**, 20677-20682.

Choi, C. K., Vicente-Manzanares, M., Zareno, J., Whitmore, L. A., Mogilner, A. and Horwitz, A. R. (2008). Actin and alpha-actinin orchestrate the assembly and maturation of nascent adhesions in a myosin II motor-independent manner. *Nat. Cell Biol.* **10**, 1039-1050.

Chu, H., Thievessen, I., Sixt, M., Lammermann, T., Waisman, A., Braun, A., Noegel, A. A. and Fassler, R. (2006). gamma-Parvin is dispensable for hematopoiesis, leukocyte trafficking, and T-cell-dependent antibody response. *Mol. Cell. Biol.* **26**, 1817-1825.

Chuang, J. Z., Lin, D. C. and Lin, S. (1995). Molecular cloning, expression, and mapping of the high affinity actin-capping domain of chicken cardiac tensin. *J. Cell Biol.* **128**, 1095-1109.

Clark, K., Pankov, R., Travis, M. A., Askari, J. A., Mould, A. P., Craig, S. E., Newham, P., Yamada, K. M. and Humphries, M. J. (2005). A specific alpha5beta1-integrin conformation promotes directional integrin translocation and fibronectin matrix formation. *J. Cell Sci.* **118**, 291-300.

Delcommenne, M., Tan, C., Gray, V., Rue, L., Woodgett, J. and Dedhar, S. (1998). Phosphoinositide-3-OH kinase-dependent regulation of glycogen synthase kinase 3 and protein kinase B/AKT by the integrin-linked kinase. *Proc. Natl. Acad. Sci. USA* **95**, 11211-11216.

Fukuda, T., Chen, K., Shi, X. and Wu, C. (2003). PINCH-1 is an obligate partner of integrin-linked kinase (ILK) functioning in cell shape modulation, motility, and survival. *J. Biol. Chem.* **278**, 51324-51333.

Geiger, B. and Bershadsky, A. (2001). Assembly and mechanosensory function of focal contacts. *Curr. Opin. Cell Biol.* **13**, 584-592.

Geiger, B., Bershadsky, A., Pankov, R. and Yamada, K. M. (2001). Transmembrane crosstalk between the extracellular matrix-cytoskeleton crosstalk. *Nat. Rev. Mol. Cell. Biol.* **2**, 793-805.

Hannigan, G. E., Leung-Hagesteijn, C., Fitz-Gibbon, L., Coppolino, M. G., Radeva, G., Filmus, J., Bell, J. C. and Dedhar, S. (1996). Regulation of cell adhesion and anchorage-dependent growth by a new beta 1-integrin-linked protein kinase. *Nature* **379**, 91-96.

Hynes, R. O. (2002). Integrins: bidirectional, allosteric signaling machines. *Cell* **110**, 673-687.

Kaverina, I., Krylyshkina, O. and Small, J. V. (1999). Microtubule targeting of substrate contacts promotes their relaxation and dissociation. *J. Cell Biol.* **146**, 1033-1044.

Kirchner, J., Kam, Z., Tzur, G., Bershadsky, A. D. and Geiger, B. (2003). Live-cell monitoring of tyrosine phosphorylation in focal adhesions following microtubule disruption. *J. Cell Sci.* **116**, 975-986.

Legate, K. R., Montanez, E., Kudlacek, O. and Fassler, R. (2006). ILK, PINCH and parvin: the tIPP of integrin signalling. *Nat. Rev. Mol. Cell. Biol.* **7**, 20-31.

Li, F., Zhang, Y. and Wu, C. (1999). Integrin-linked kinase is localized to cell-matrix focal adhesions but not cell-cell adhesion sites and the focal adhesion localization of integrin-linked kinase is regulated by the PINCH-binding ANK repeats. *J. Cell Sci.* **112**, 4589-4599.

Li, S., Bordoy, R., Stanchi, F., Moser, M., Braun, A., Kudlacek, O., Wewer, U. M., Yurchenco, P. D. and Fassler, R. (2005). PINCH1 regulates cell-matrix and cell-cell adhesions, cell polarity and cell survival during the peri-implantation stage. *J. Cell Sci.* **118**, 2913-2921.

Lo, S. H., Janmey, P. A., Hartwig, J. H. and Chen, L. B. (1994). Interactions of tensin with actin and identification of its three distinct actin-binding domains. *J. Cell Biol.* **125**, 1067-1075.

Mackinnon, A. C., Qadota, H., Norman, K. R., Moerman, D. G. and Williams, B. D. (2002). C. elegans PAT-4/ILK functions as an adaptor protein within integrin adhesion complexes. *Curr. Biol.* **12**, 787-797.

Maubant, S., Saint-Dizier, D., Boutillon, M., Perron-Sierra, F., Casara, P. J., Hickman, J. A., Tucker, G. C. and Van Obberghen-Schilling, E. (2006). Blockade of alpha v beta3 and alpha v beta5 integrins by RGD mimetics induces anoikis and not integrin-mediated death in human endothelial cells. *Blood* **108**, 3035-3044.

Naviaux, R. K., Costanzi, E., Haas, M. and Verma, I. M. (1996). The pCL vector system: rapid production of helper-free, high-titer, recombinant retroviruses. *J. Virol.* **70**, 5701-5705.

Nikolopoulos, S. N. and Turner, C. E. (2001). Integrin-linked kinase (ILK) binding to paxillin LD1 motif regulates ILK localization to focal adhesions. *J. Biol. Chem.* **276**, 23499-23505.

Nikolopoulos, S. N. and Turner, C. E. (2002). Molecular dissection of actopaxin-integrin-linked kinase-Paxillin interactions and their role in subcellular localization. *J. Biol. Chem.* **277**, 1568-1575.

Pankov, R., Cukierman, E., Katz, B. Z., Matsumoto, K., Lin, D. C., Lin, S., Hahn, C. and Yamada, K. M. (2000). Integrin dynamics and matrix assembly: tensin-dependent translocation of alpha(5)beta(1) integrins promotes early fibronectin fibrillogenesis. *J. Cell Biol.* **148**, 1075-1090.

Sakai, T., Li, S., Docheva, D., Grashoff, C., Sakai, K., Kostka, G., Braun, A., Pfeifer, A., Yurchenco, P. D. and Fassler, R. (2003). Integrin-linked kinase (ILK) is required for polarizing the epiblast, cell adhesion, and controlling actin accumulation. *Genes Dev.* **17**, 926-940.

Silver, D. P. and Livingston, D. M. (2001). Self-excising retroviral vectors encoding the Cre recombinase overcome Cre-mediated cellular toxicity. *Mol. Cell* **8**, 233-243.

Stanchi, F., Bordoy, R., Kudlacek, O., Braun, A., Pfeifer, A., Moser, M. and Fassler, R. (2005). Consequences of loss of PINCH2 expression in mice. *J. Cell Sci.* **118**, 5899-5910.

Torgler, C. N., Narasimha, M., Knox, A. L., Zervas, C. G., Vernon, M. C. and Brown, N. H. (2004). Tensin stabilizes integrin adhesive contacts in Drosophila. *Dev Cell* **6**, 357-369.

van der Flier, A. and Sonnenberg, A. (2001). Function and interactions of integrins. *Cell Tissue Res.* **305**, 285-298.

Vouret-Craviari, V., Boulter, E., Grall, D., Matthews, C. and Van Obberghen-Schilling, E. (2004). ILK is required for the assembly of matrix-forming adhesions and capillary morphogenesis in endothelial cells. *J. Cell Sci.* **117**, 4559-4569.

Wang, X., Fukuda, K., Byeon, I. J., Velyvis, A., Wu, C., Gronenborn, A. and Qin, J. (2008). The structure of alpha-parvin CH2-paxillin LD1 complex reveals a novel modular recognition for focal adhesion assembly. *J. Biol. Chem.* **283**, 21113-21119.

Wu, C. (2004). The PINCH-ILK-parvin complexes: assembly, functions and regulation. *Biochim. Biophys. Acta* **1692**, 55-62.

Yamaji, S., Suzuki, A., Sugiyama, Y., Koide, Y., Yoshida, M., Kanamori, H., Mohri, H., Ohno, S. and Ishigatsubo, Y. (2001). A novel integrin-linked kinase-binding protein, affixin, is involved in the early stage of cell-substrate interaction. *J. Cell Biol.* **153**, 1251-1264.

Yoshigi, M., Hoffman, L. M., Jensen, C. C., Yost, H. J. and Beckerle, M. C. (2005). Mechanical force mobilizes zyxin from focal adhesions to actin filaments and regulates cytoskeletal reinforcement. *J. Cell Biol.* **171**, 209-215.

Zaidel-Bar, R., Ballestrem, C., Kam, Z. and Geiger, B. (2003). Early molecular events in the assembly of matrix adhesions at the leading edge of migrating cells. *J. Cell Sci.* **116**, 4605-4613.

Zaidel-Bar, R., Milo, R., Kam, Z. and Geiger, B. (2007). A paxillin tyrosine phosphorylation switch regulates the assembly and form of cell-matrix adhesions. *J. Cell Sci.* **120**, 137-148.

Zamir, E., Katz, B. Z., Aota, S., Yamada, K. M., Geiger, B. and Kam, Z. (1999). Molecular diversity of cell-matrix adhesions. *J. Cell Sci.* **112**, 1655-1669.

Zamir, E., Katz, M., Posen, Y., Erez, N., Yamada, K. M., Katz, B. Z., Lin, S., Lin, D. C., Bershadsky, A., Kam, Z. et al. (2000). Dynamics and segregation of cell-matrix adhesions in cultured fibroblasts. *Nat. Cell Biol.* **2**, 191-196.

Zervas, C. G., Gregory, S. L. and Brown, N. H. (2001). Drosophila integrin-linked kinase is required at sites of integrin adhesion to link the cytoskeleton to the plasma membrane. *J. Cell Biol.* **152**, 1007-1018.

Zhang, Y., Chen, K., Tu, Y., Velyvis, A., Yang, Y., Qin, J. and Wu, C. (2002). Assembly of the PINCH-ILK-CH-ILKBP complex precedes and is essential for localization of each component to cell-matrix adhesion sites. *J. Cell Sci.* **115**, 4777-4786.

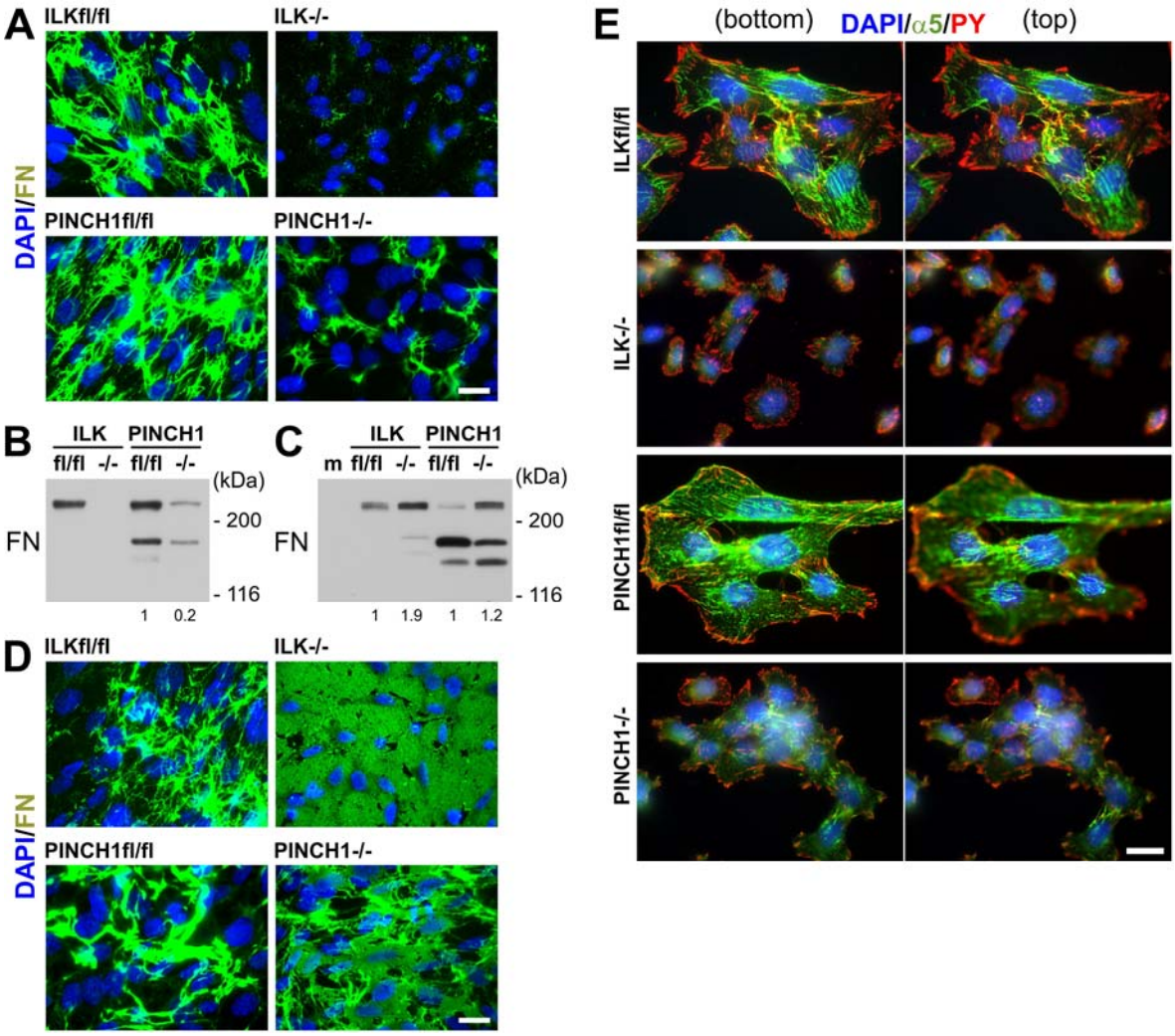

Fig. S1. Defective fibronectin assembly due to impaired formation of FB after ILK or PINCH1 deletion. [A] Impact of ILK of PINCH1 deletion on the assembly of endogenous FN, which is detected either by fluorescent staining of non-permeabilized cells cultured on glass coverslips (A) or by western blot analysis of deoxycholate (DOC)-insoluble cell extracts (B). [C] Endogenous FN is however secreted by the knock-out cells and it accumulates in the culture medium; m = control medium. Intensities of the sum of the bands in -/- samples relative to the sum of the bands in fl/fl samples, as determined by densitometry analysis, are indicated below. [D] ILK or PINCH1 deletion impacts also on the ability of the cells to remodel surface-adsorbed FN, as detected by immunofluorescent anti-FN antibody staining of cells cultured on FN-coated coverslips. [E] ILK or PINCH1 deletion impaires FB formation. Cells on coverslips were stained with anti-integrin α_5 (FB marker) and anti-PY (FX and FA marker) antibodies. Images represent the lower surface of cells in contact with the substrate (bottom), or their upper surface (top). All experiments were performed 20 hours after plating the cells. All bars = 20 μm.

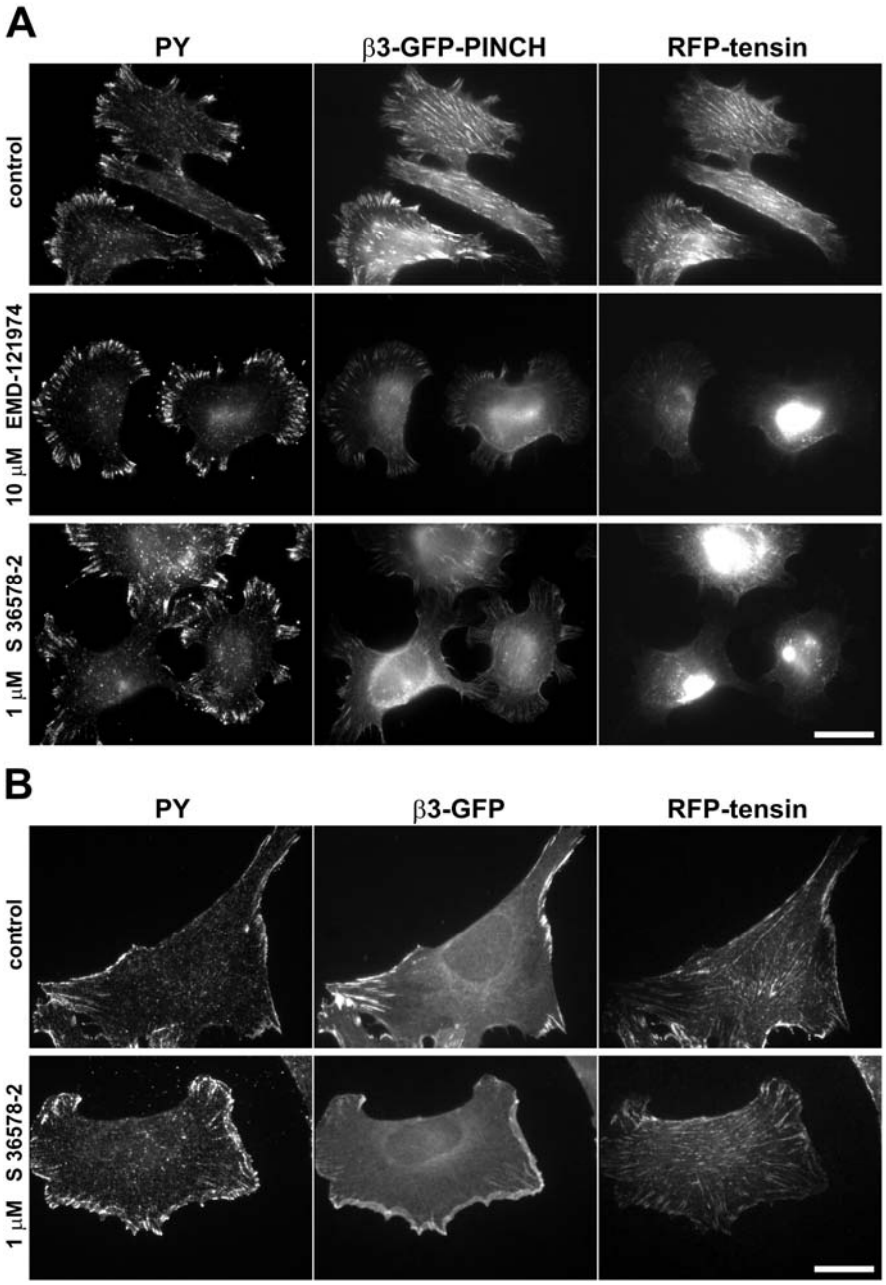

Fig. S2. The β3-GFP-IPP chimera function as αvβ3 heterodimers. [A] Treatment of PINCH1T-/- cells expressing β_3-GFP-PINCH with the α_v integrin-specific inhibitors EMD-121974 or S-36578- 2 (identical results were obtained in cells expressing β_3-GFP-ILK and β_3-GFP-parvin). [B] Analogous treatment in PINCH1fl/fl cells. All cells were suspended in medium in absence or presence of the inhibitor, plated on coverslips coated with 50 ng/ml vitronectin + 500 ng/ml FN, fixed and stained with anti-PY antibody. Bars = 20 μm.

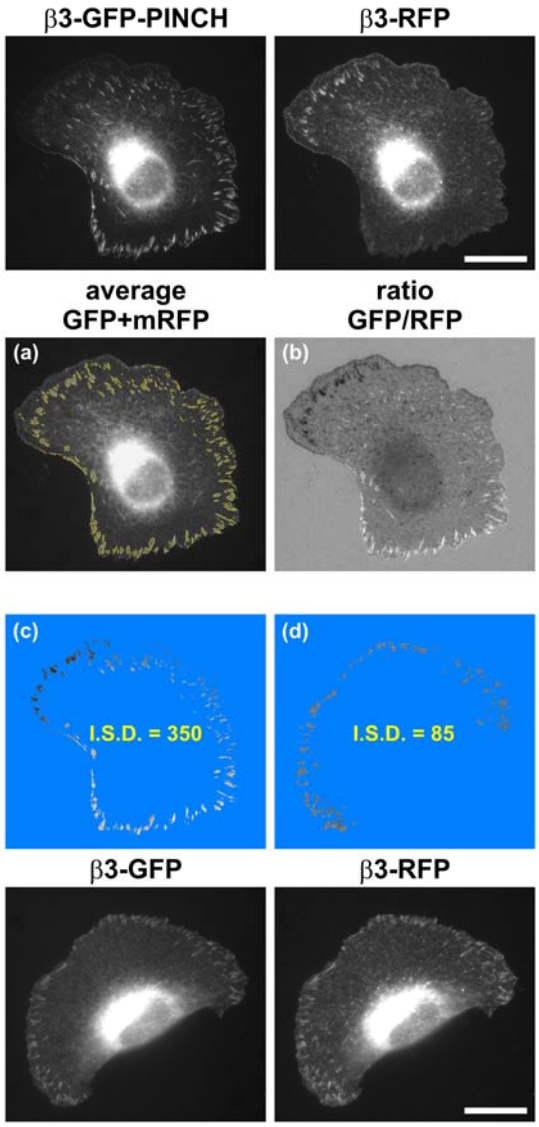

Fig. S3. Quantification of different localization of the β3-GFP-IPP chimeras with respect to the internal control β3-RFP. Example of the procedure for a 3T3/ β_3-RFP cell co-expressing β_3-GFP-PINCH. The arithmetic functions of Metamorph are used to build a 16 bit average image and a 16 bit ratio image (obtained by dividing the GFP signal multiplied by 1000 with the RFP signal). Regions to analyze (adhesions positives for RFP and/or GFP signals) are selected in the average image using the threshold function (a) and excluding manually the region corresponding to the highly fluorescent perinuclear area. The selected regions are then applied to the ratio image (b), in which light and dark grey areas correspond respectively to high and low ratio GFP/RFP. Intensity standard deviation (I.S.D.) of the whole adhesion area is read after transferring (with a script) the image within the regions of interest to an image with a black background (c) in which the area surrounding the adhesions could be excluded from the analysis upon thresholding (in light blue) to intensity >1. (d) The final output is shown after applying the same procedure to a 3T3/ β_3-RFP cell co-expressing the β_3-GFP control, in which the uniform ratio GFP/RFP overall the adhesions generates a uniform gray color and low I.S.D. (original GFP and RFP images are shown below). Bar = 20 μm. The maximum possible error of the system (system background noise I.S.D.) was calculated as sum of GFP and RFP background noise I.S.D.s, obtained by analyzing sets of two sequential images in the same channel (respectively GFP or RFP).

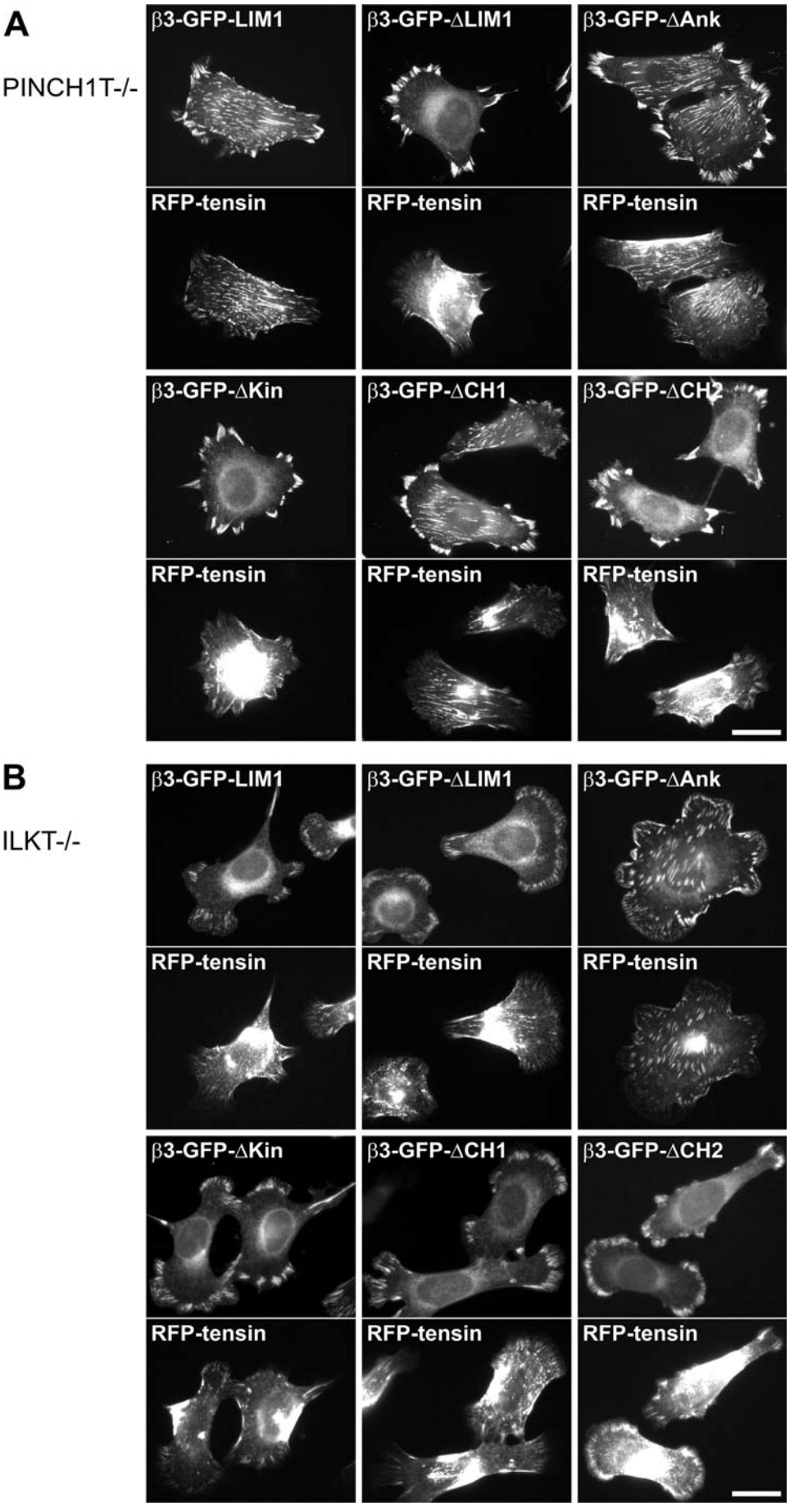

Fig. S4. Different effects of the β_3-GFP-IPP chimera deletion mutants on the formation of tensin-rich adhesions in PINCH1-null or ILK-null backgrounds. Representative images of PINCH1T-/- cells (A) and ILKT-/- cells (B) expressing each β_3-GFP-IPP chimera deletion mutant. Cell were fixed 4 hours after plating on uncoated coverslips. Bars= 20 μm.